FIFTH INTERNATIONAL CONGRESS ON SOUND AND VIBRATION
DECEMBER 15-18, 1997
ADELAIDE, SOUTH AUSTRALIA

A METHOD TO CORRECT THE 3D ACTIVE AND REACTIVE SOUND INTENSITY VECTORS USING A ROTATING 1D PROBE IN AN UNSTEADY ACOUSTIC FIELD

***C. PICARD, J.C. PATRAT, A. DURAN, **H.S. NA, *J.C. REBILLAT**

*LEA, 43 route de l'aérodrome, 86036 POITIERS CEDEX
**KHRC, Kumhwa Bldg, 16F, 949-1, Togok-Dong, Kangnam-gu, SEOUL 135-270, Korea

ABSTRACT

A well-known unidirectional probe to which a rotating motion is imparted can measure the three components of the sound intensity vector. Such a sequential measurement procedure produces some scattering and bias errors when the acoustic field is unsteady. During the measurement period, the magnitude of the physical phenomenon is supposed to vary but not its geometric properties. This leads to a simple calculation of these errors and an optimal estimation of the sound power level of the source which is used to correct the active and the reactive sound intensity vectors. For a random steady field, the same method of correction reduces the scattering of the measurements. Theoretical and experimental studies under laboratory conditions verify the effect of the correction even in a reactive field. We also show that in the case of noise emission by a short-duration supersonic jet, the same scattering reduction thus allows a more accurate localization of the intensity vectors.

I. INTRODUCTION

Several technological solutions [1] [2] have been proposed to measure the three components of the sound intensity vector. The simplest solution [3] [4] use a classical two-microphone probe fixed on a rotative support according to the design of figure 1. The support rotation axis presents a characteristic angle of 54.74° with the measurement axis defined by the two microphones. Thus, two rotations of 120° around the support axis allow orienting successively the microphone axis at the three orthogonal directions of the measurement axis system.

For each axis, the components of the active and reactive sound intensity vectors are classically determined [5] using the pressure auto-spectra and cross-spectrum. The acoustic field being rarely steady, this sequential measurement procedure produces some biases (figure 2), which depend on the probe orientation. A quick study of these measurement biases allows calculating the maximum errors.

A local and optimum estimation of the acoustic power level of the source is used to correct the measurement biases as much for the active intensity as for the reactive intensity.

Two kinds of presentation of the results are proposed. These layouts make easier the interpretation of the directions of the intensity vectors and, for simple acoustic situations, help for the localization of the sound sources.

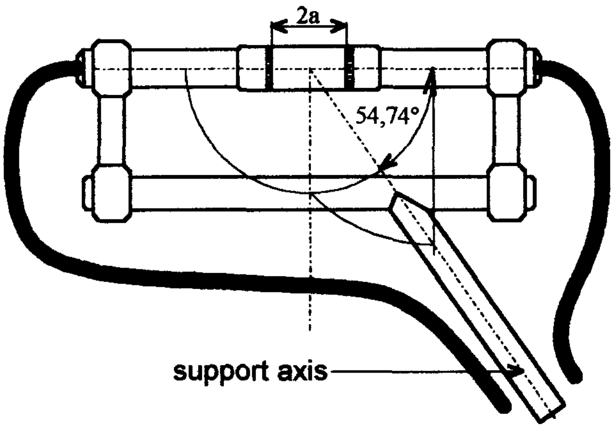

Figure 1 : Probe diagram

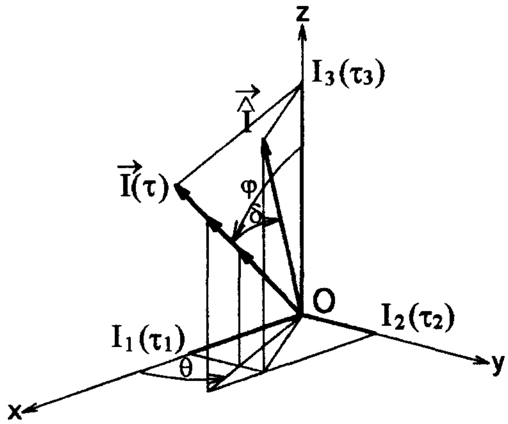

Figure 2 : Erroneous vector

II. SEQUENTIAL MEASUREMENT

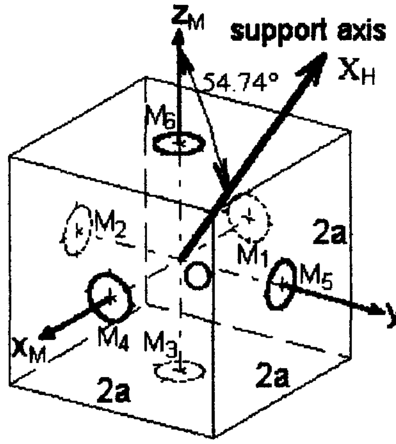

Figure 3 : Positions of the microphones

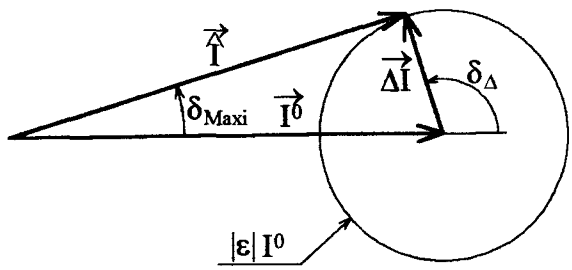

Figure 4 : Maximum errors

During the measurement sequence, the two rotations of 120° carry the two microphones of the probe with a circular permutation according to figure 3.
Using this notation, an axis marked m is defined by the M_m and M_{m+3} microphones. Thus the x-axis corresponds to $m = 1$, y-axis to $m = 2$ and z-axis to $m = 3$.
Within the scope of the finite differences approximation, each component Ia_m or Ir_m is obtained by means of the spectrum functions :

- active sound intensity

$$Ia_m(\omega,\tau_m) = -\frac{1}{2a\rho\omega}\Im m\left[G_{m,m+3}(\omega,\tau_m)\right] \qquad (1)$$

Where the $G_{m,m+3}(\omega,\tau_m)$, averaged cross-spectra (temporal scale t), are representative of the phenomena at a τ_m date characterizing the measuring sequence m.
The source power levels at the τ_1, τ_2 and τ_3 dates being different, the sequential measurements lead to an erroneous vector $\vec{\tilde{I}}$ as shown in figure 2.

- reactive sound intensity

$$Ir_m(\omega,\tau_m)=\frac{G_{m,m}(\omega,\tau_m)-G_{m+3,m+3}(\omega,\tau_m)}{4a\rho\omega} \tag{2}$$

With the same comments as above.

III. SEQUENTIAL ERRORS

The study of the errors introduced by the sequential measurement of pressures requires characterizing the noise source. This is supposed to be general but its mean acoustic power varies slowly in time. Under this assumption [3] the intensity vector orientation defined by the θ and φ angles of figure 2, doesn't change in terms of the mean time τ_m, only its modulus does.

Choosing the measurement sequence in the *y-z-x* order with the origin of time $\tau_3=0$, corresponding to the median measurement *z*, and the same time interval $\Delta\tau$ between two consecutive measurements, the components $I_m(\tau_m)$ of the intensity vector $\vec{I}$, active or reactive are written:

$$\begin{aligned}
I_1(\tau_1)&=I_1(\omega,\Delta\tau)=(1+\varepsilon)\,I_1^0=(1+\varepsilon)\,I^0\sin\varphi\cos\theta\\
I_2(\tau_2)&=I_2(\omega,-\Delta\tau)=(1-\varepsilon)\,I_2^0=(1-\varepsilon)\,I^0\sin\varphi\sin\theta\\
I_3(\tau_3)&=I_3(\omega,0)=I_3^0=I^0\cos\varphi
\end{aligned} \tag{3}$$

Where ε, representing the relative variation of the source power between two consecutive measurements, verifies $|\varepsilon|<<1$ and where $\vec{I}^0=\vec{I}(\tau_3)$ is the reference vector.

The measurement biases falling to the sequential measurements correspond to three errors on the determination of the intensity vector: one error on the modulus and two errors on the orientation. The only physically interesting error is the angle δ of figure 2 because it doesn't depend on the probe orientation.

Therefore the measurement biases are characterized by the two following coefficients :

$$g=\frac{\|\vec{I}\|}{\|\vec{I}^0\|}=\sqrt{1+\varepsilon\,(\varepsilon+2\cos 2\theta)\sin^2\varphi} \tag{4}$$

$$\cos\delta=\frac{1+\varepsilon\sin^2\varphi\cos 2\theta}{\sqrt{1+2\varepsilon\sin^2\varphi\cos 2\theta+\varepsilon^2\sin^2\varphi}}$$

Or we can study the variation of $\vec{\Delta I}=\vec{I}-\vec{I}^0$, thanks to :

$$\begin{aligned}
g_\Delta&=|\varepsilon|\sin\varphi\\
\cos\delta_\Delta&=sign(\varepsilon)\sin\varphi\cos 2\theta \qquad \text{for } \varphi\neq 0,\pi
\end{aligned} \tag{5}$$

In these conditions the end of the vector $\vec{I}$ is in a sphere centered at the end of the vector $\vec{I}^0$ and with a radius $|\varepsilon|\,I^0<<I^0$.

The ideal stationary assumption of the theory being hardly possible in industrial cases, it's important to search some correction procedures.

IV. CORRECTION METHOD

The source and acoustic field hypotheses lead to :

- the phase $\phi_{m,m+3}(\omega)$ of the cross-spectrum depends on the geometry and the random nature of the source as well as on the position and the orientation of the probe,

- the modulus $\left|G_{m,m+3}(\omega,\tau_m)\right|$ is, moreover, modulated by the source power level.

So, the correction of the measurements requires looking for an estimation of the source power level for every date τ_m.

The pressure auto-spectrum measured at any point of space is such estimation. The estimation at the point P, center of the probe and theoretical point of the measurement, is the optimal estimation since this point remains unchanged during the rotations of the probe. His value is deduced from the measurements by the finite differences approximation :

$$G_{pp}(\omega,\tau_m)=\tfrac{1}{4}\left(G_{m,m}(\omega,\tau_m)+G_{m+3,m+3}(\omega,\tau_m)+2\Re e\left[G_{m,m+3}(\omega,\tau_m)\right]\right)\quad(6)$$

This estimation of the source power level allows the corrections of the acoustic intensity vectors (active and reactive).

The components of the corrected vector $\vec{\tilde{I}}$ are defined, at the intermediate date τ_z of the y-z-x sequence, by :

$$\begin{aligned}\tilde{I}_x(\omega,\tau_z)&=I_x(\omega,\tau_x)\frac{G_{pp}(\omega,\tau_z)}{G_{pp}(\omega,\tau_x)}\\ \tilde{I}_y(\omega,\tau_z)&=I_y(\omega,\tau_y)\frac{G_{pp}(\omega,\tau_z)}{G_{pp}(\omega,\tau_y)}\\ \tilde{I}_z(\omega,\tau_z)&=I_z(\omega,\tau_z)\end{aligned}\quad(7)$$

V. DISPLAY TECHNIQUES

It is not easy to show on a graph the variation in orientation of an acoustic intensity vector as a function of frequency. Two graphic representations have been designed to make the interpretation easier in terms of sources localization if this is justified.

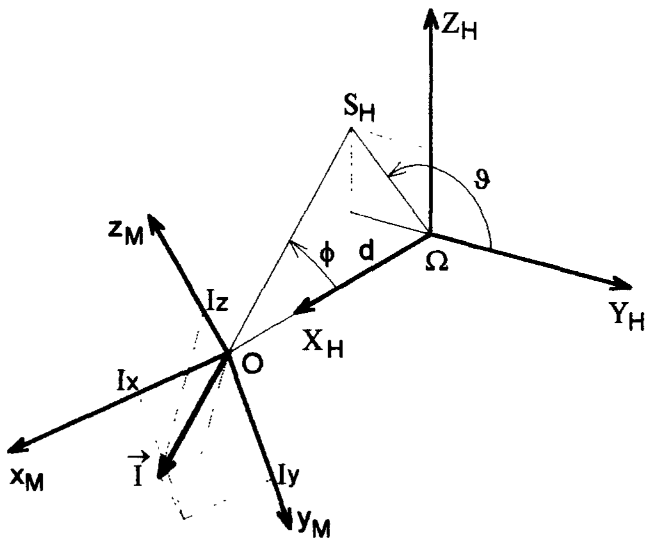

Figure 5 : Location of the vector $\vec{I}$

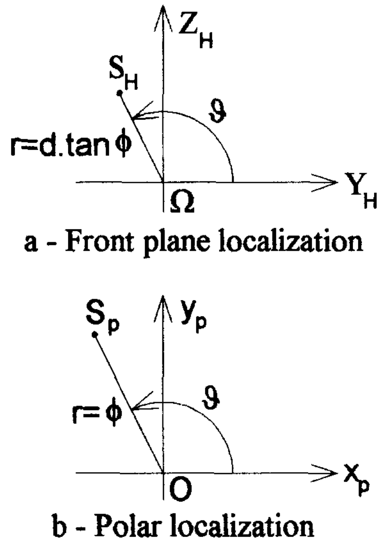

Figure 6 : Display techniques

The two techniques is based on the geometrical elements of figure 5 where $(O;x_M,y_M,z_M)$ is the measurement axis system defined by the microphones and $(\Omega;X_H,Y_H,Z_H)$ is an axis system tied to the probe support which the $O\Omega$ -axis is the axis of rotation.

First method: Projection onto a front-plane [3] figure 6-a. One associate the $\vec{I}$ vector to the point S_H of the plane $(\Omega;X_H,Y_H)$.
Second method: Polar representation figure 6-b. The orientation of the vector $\vec{I}$ is defined by the angles $\vartheta \in]-\pi,\pi]$ and $\phi \in [0,\pi]$ to which one associate the point S_p of the display plane $(O;x_p,y_p)$.

VI. EXPERIMENTAL DEVICES

The experiments have been realized with the help of two different systems.
- The first system uses the diagram drawn in figure 7. It resumes the one of [6] and allows a comparison with a simple theoretical approach. Three speakers spaced out of $D = 18$cm are activated by a white noise with the central speaker in opposite phase. The rotative probe, $2a = 12$mm, takes place at the point $O = (D, -\frac{1}{3}D, -D)$. The measurement frequency range is from 125Hz to 7500Hz with a step of 6.25Hz for three levels reproduced for each of the three probe orientation. This ensures to study three steady power rates and six variable power rates.
- The second experiment uses the test-bed called MARTEL [7][8]. This system is designed to study the supersonic jet noise emission of spatial launchers as Ariane 5. The experimental device is described in figure 8.

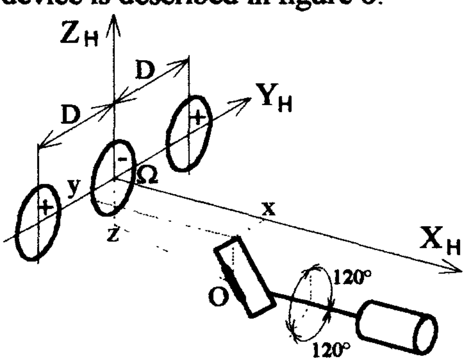

Figure 7 : 3 speakers experimental device

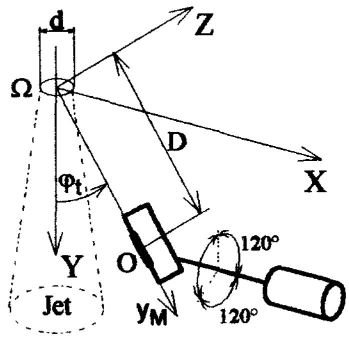

Figure 8 : Supersonic jet

VII. THEORETICAL STUDY

A very simple modeling of the device of figure 7 is to replace the three speakers by single-polar sources of forces $(+A,-A,+A)$. The acoustic field thus created is very complicated [6]. At every point of space, some singular frequencies appear for which the finite differences approximation can be put in flaws.
At the measurement point O the active and reactive acoustic intensities are calculated for $A=1$. The sequential measurements using the rotative probe are simulated by fixing $A = 1/\sqrt{2}$ for the y_M-axis, $A=1$ for the z_M-axis and $A=\sqrt{2}$ for x_M-axis. This corresponds to 3dB gaps of the power level of the single-polar sources.
The figure 9 shows the errors on the levels of the corrected LIaDFC, LIrDFC, uncorrected LIaDF, LIrDF and real intensities LIa, LIr.
The figure 10 shows the angular errors δaDF, δrDF, δaDFC, δrDFC between the uncorrected, corrected and real vectors.
These curves reveal the interest of the proposed correction method. They also shows that the finite differences can be used beyond the conventional high frequency boundary, that is 5200 Hz

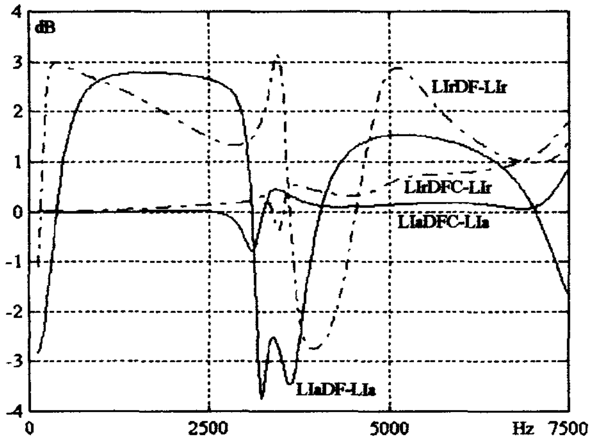

Figure 9 – Levels errors

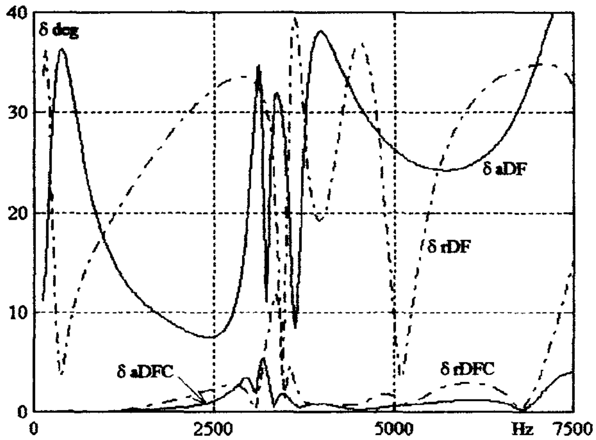

Figure 10 – Incidences errors

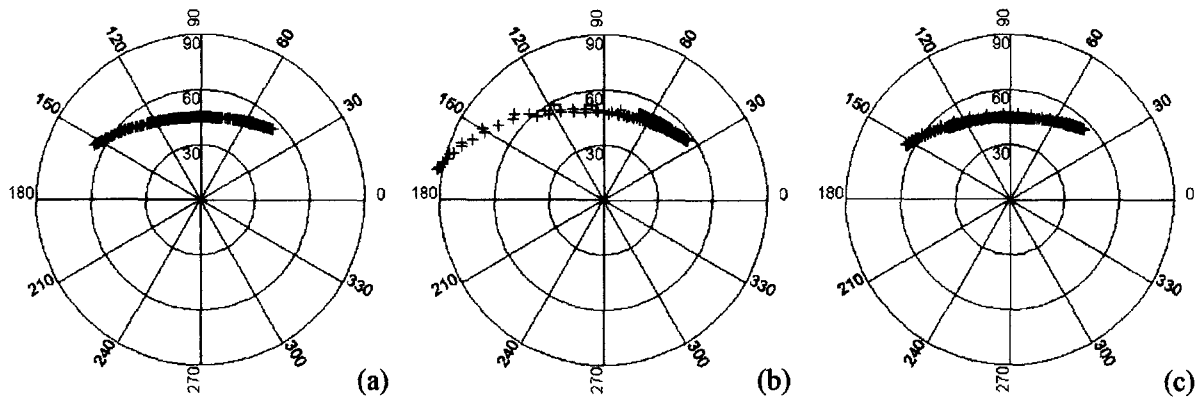

Figures 11 – Active acoustic intensity : (a) real, (b) uncorrected, (c) corrected

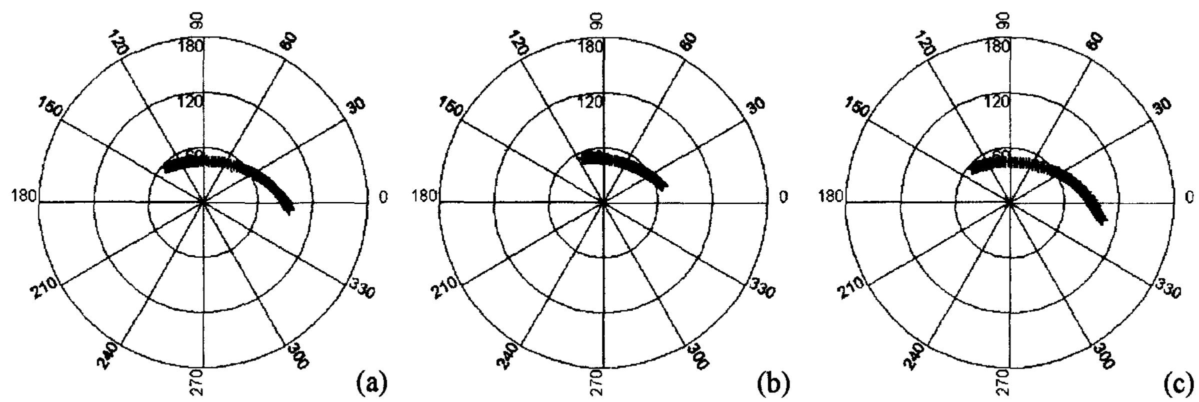

Figures 12 - Reactive acoustic intensity : (a) real, (b) uncorrected, (c) corrected

The figures 11 et 12 show the acoustic intensities according to the display technique of figure 6-b. They give proof of the efficiency of the correction method in presence of a strongly variable field. Some gaps with the real values still remain which is a consequence of the finite differences principle.

VIII. EXPERIMENTAL RESULTS

The experiments carried out using the system of figure 7 are similar to the previous theoretical study. However, it would be unwise to compare the two because the experimental conditions are very far from the theoretical model. On the other hand, a comparison is possible between the experimental results under uncorrected (figure 13-a and 14-a), corrected variable power

state (figure 13-b and 14-b) and uncorrected steady power state (figure 13-c and 14-c) which can be the reference.
The correction method cancels the errors due to the source power level fluctuations during the sequential measurements.

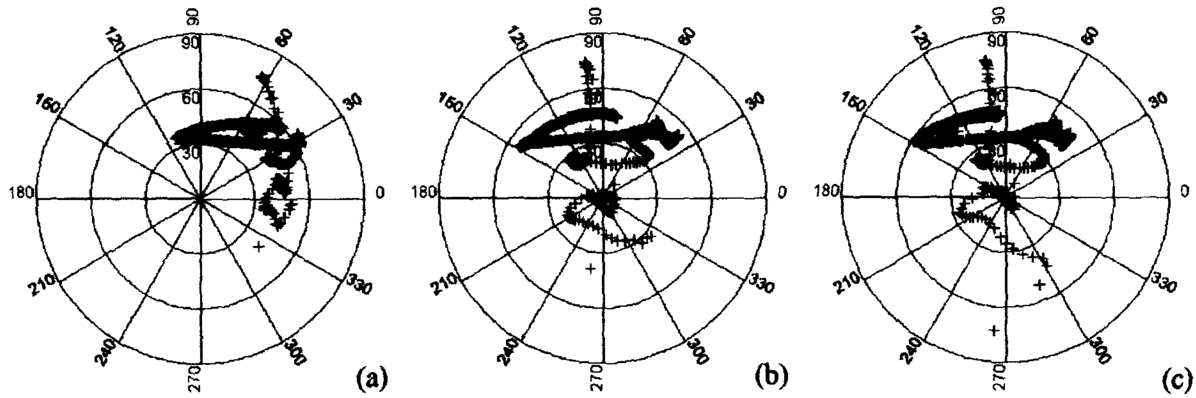

Figures 13 - Active intensity : (a) uncorrected variable, (b) corrected variable, (c) steady

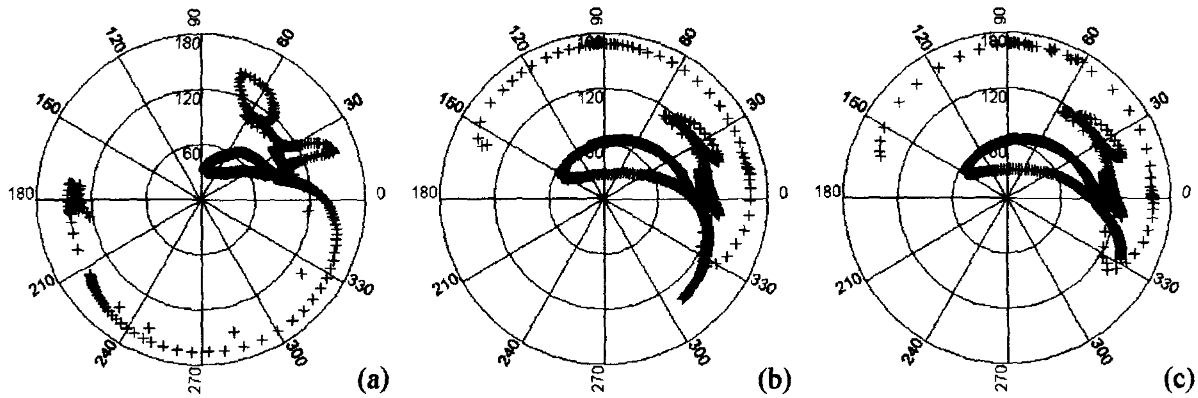

Figures 14 - Reactive intensity : (a) uncorrected variable, (b) corrected variable, (c) steady

The experiment driven on the MARTEL test-bed according to the device of figure 8, have the following geometrical characteristics : $D = 60d$, $\varphi_t = 90°$, a nozzle diameter $d = 60mm$. The jet characteristics are : a mean velocity $v = 1200m/s$, a mean temperature $T = 428K$ and a Mach number $M = 2.84$. In consideration of the high cost of a blast, the duration of the sequential data acquisition is limited to 35s. The spectral analysis is made up to 10kHz with a step of 25Hz and 100 averages.
The displaying principle of figure 6-b is applied to figures 15-a (uncorrected active intensity) and 15-b (corrected active intensity).

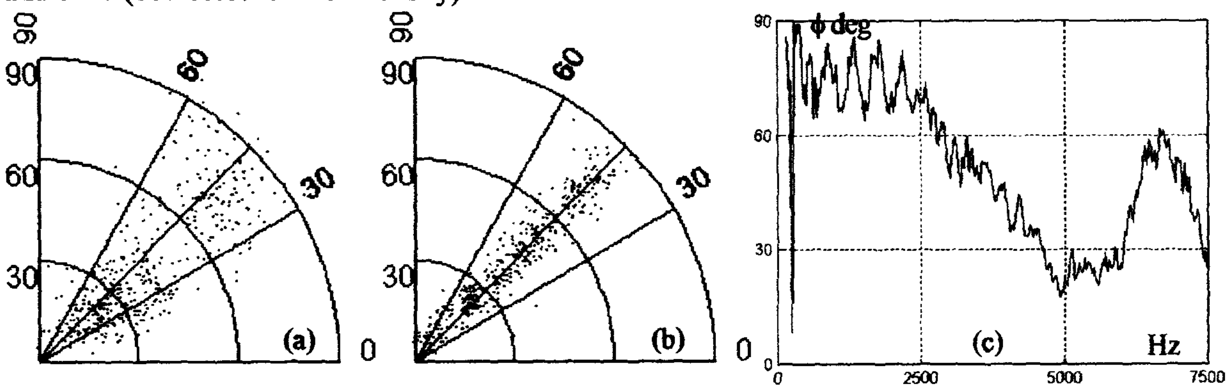

Figures 15 - Jet measurement : (a) uncorrected, (b) corrected, (c) incidence

The correction reduces the scattering errors. The acoustic field being strongly random, everything goes as if a power level fluctuation would exist between each sequential acquisition. The angle $\vartheta \approx 45°$ corresponds to the symmetric plane of the jet. The clustering of points around this axis gives a more physical meaning of the jet noise emission. In this plane, it is then possible to study the directivity of the acoustic field, angle ϕ, as a function of frequency, figure 15-c. But this work is not relevant to jet noise emission study.

IX. CONCLUSION

The theoretical analysis of the effects of the measurements sequential procedure leads to a valuation of the errors for weak fluctuations of the acoustic source power level. Thus a 1dB variation can conduct to an orientation error of 15°. In the presence of strong variations, the measurements loose their sense and it is imperative to correct them.
The pressure auto-spectrum calculated at the probe center is the best estimation of the local power level of the source and permits a simple correction of measurements.
A numerical simulation and various experiments have validated the efficiency of the correction method. The advantage of the correction even extends to random stationary fields.
Our 1D rotative and 3D spherical probes [9] [10] are both complementary. A comparative study is in progress.

REFERENCES

[1] Yanagisawa, T., Koike, N., Cancellation of both phase mismatch and position errors with rotating microphones in sound intensity measurement. J. Sound Vib. 113 (1) [1987], 117-126.

[2] Nishida, K., Kubota, Y., Hayashi, S., Tomita, T., Errors in the automatic measurement of spatial acoustic intensity in the direction of sound energy propagation with a rotating probe. J. Sound Vib. 138 (1) [1990], 1-15.

[3] Rébillat, J.C., Patrat, J.C., Picard, C., Intensimétrie tridimensionnelle avec une sonde rotative à deux microphones. ACUSTICA - acta acustica Vol 83 (1997) 342-353.

[4] Patrat, J.C., Picard, C., Rébillat, J.C., NA H.S., Mesures sequentielles des trois composantes des intensités acoustiques active et réactive en présence de fortes fluctuations du champ acoustique. 13ème Congrès Français de Mécanique (AUM), Poitiers Futuroscope, 1-5 septembre 1997.

[5] Fahy, F. J., Sound Intensity. Elsevier 1990.

[6] Tichy, J., Adin Man III, J., Use of the complex intensity for sound radiation and sound field studies. Proc. 2nd Int. Congress Acoustic Intensity. Senlis [1985], 113-120.

[7] Foulon H., MARTEL : Moyen Aéroacoustique de Recherche et Technologie sur l'Environnement des Lanceurs. Nouvelle Revue d'Aéronautique et d'Astronautique - N°3 - 1997, .

[8] Foulon H., Peube J. L., Rebillat J. C., Moyens d'essais pour l'étude aéroacoustique de jets supersoniques : banc MARTEL.CNES ONERA International conference on "acoustic and dynamic environment of space transportation systems". Jouy-en-Josas [1994], 351-358

[9] Coste, O., Patrat, J. C., Diffraction autour d'une sphère appliquée à une sonde intensimétrique 3D. 1er Congrès Français d'Acoustique, Lyon 1990, J. Phys. II [1990], C2 895-898

[10] Coste, O., Patrat, J. C., Scattering of a spherical wave applied to a 3D sound intensity probe. Internoise 1991, Sydney, [1991], 1017-1020